

1 **A dual-application poly (DL-lactic-co-glycolic) acid (PLGA)-chitosan composite scaffold**  
2 **for potential use in bone tissue engineering**

3 Yamina Boukari<sup>a</sup> ([yamina.boukari@gmail.com](mailto:yamina.boukari@gmail.com)), Omar Qutachi<sup>b</sup>  
4 (omar.qutachi@nottingham.ac.uk), David J. Scurr<sup>b</sup> ([david.scurr@nottingham.ac.uk](mailto:david.scurr@nottingham.ac.uk)), Andrew  
5 P. Morris<sup>a</sup> ([andrew.morris@nottingham.edu.my](mailto:andrew.morris@nottingham.edu.my)), Stephen W. Doughty<sup>c</sup>  
6 (stephen.doughty@pmc.edu.my), and Nashiru Billa<sup>a\*</sup>

7 <sup>a</sup>School of Pharmacy, The University of Nottingham Malaysia Campus, Jalan Broga, 43500  
8 Semenyih, Selangor, Malaysia.

9 <sup>b</sup>School of Pharmacy, The University of Nottingham, Park Campus, Nottingham NG7 2RD,  
10 United Kingdom.

11 <sup>c</sup>Penang Medical College, 4 Jalan Sepoy Lines, 10450 George Town, Penang, Malaysia

12 \*Corresponding author: [Nashiru.Billa@nottingham.edu.my](mailto:Nashiru.Billa@nottingham.edu.my); Tel, +60389248211; Fax,  
13 +60389248018

14

15

16

17

18

19

20

21

22 **Abstract**

23 The development of patient-friendly alternatives to bone-graft procedures is the driving force  
24 for new frontiers in bone tissue engineering. Poly (DL-lactic-co-glycolic acid), (PLGA) and  
25 chitosan are well-studied and easy-to-process polymers from which scaffolds can be  
26 fabricated. In this study, a novel dual-application scaffold system was formulated from  
27 porous PLGA and protein-loaded PLGA/chitosan microspheres. Physicochemical and *in vitro*  
28 protein release attributes were established. The therapeutic relevance, cytocompatibility with  
29 primary human mesenchymal stem cells (hMSCs) and osteogenic properties were tested.  
30 There was a significant reduction in burst release from the composite PLGA/chitosan  
31 microspheres compared with PLGA alone. Scaffolds sintered from porous microspheres at  
32 37°C were significantly stronger than the PLGA control, with compressive strengths of 0.846  
33 ± 0.272 MPa and 0.406 ± 0.265 MPa, respectively (p < 0.05). The formulation also sintered at  
34 37°C following injection through a needle, demonstrating its injectable potential. The  
35 scaffolds demonstrated cytocompatibility, with increased cell numbers observed over an 8-  
36 day study period. Von Kossa and immunostaining of the hMSC-scaffolds confirmed their  
37 osteogenic potential with the ability to sinter at 37°C *in situ*.

38 Keywords: polymeric biomaterials, controlled delivery, poly (lactic-co-glycolic acid)  
39 (PLGA), microspheres, protein delivery, tissue engineering, mechanical properties,  
40 formulation.<sup>1</sup>

---

<sup>1</sup>Abbreviations

BMPs, bone morphogenetic proteins; BSA, bovine serum albumin; DCM, dichloromethane; DMSO, dimethyl sulphoxide; ECM, extracellular matrix; FTIR, Fourier transform infrared; hMSC, primary human mesenchymal stem cells; PBS, phosphate-buffered saline; PLGA, poly (lactic-co-glycolic acid); PVA, poly (vinyl alcohol); SDS, sodium dodecyl sulphate; SEM, scanning electron microscopy, TPP, sodium tripolyphosphate; ToF-SIMS, time of flight secondary ion mass spectroscopy.

## 41 **1. Introduction**

42 There is an urgent need for alternative approaches for the regeneration of bone  
43 following fracture or orthopaedic damage *in lieu* of traditional methods, and these alternative  
44 approaches constitute an important tissue engineering application (Vo et al., 2012). The  
45 current ‘gold standard’ therapy is the bone graft procedure, which involves taking autologous  
46 bone, usually harvested from the iliac crest of the patient, and implanting it into their defect  
47 site (Martino et al., 2012; Amini et al., 2013). Alternatively, allograft bone from donors or  
48 cadavers can be extracted from the femoral heads or extremities of other long bones (Delloye  
49 et al., 2007). This implanted tissue acts as a scaffold for the existing bone tissue to infiltrate  
50 and deposit extracellular matrix (ECM), leading to the remodelling of the fractured bone  
51 (Bostrom and Mikos, 1997). Numerous drawbacks are associated with the above procedures,  
52 including the limited supply of autologous bone, complications at the donor site and high  
53 surgical costs (Martino et al., 2012). Furthermore, in large defects, resorption may occur  
54 before osteogenesis has been completed (Burg et al., 2000). Allograft bone usage is associated  
55 with incompatibility with the host, and the possible transmission of diseases and infections  
56 such as hepatitis and HIV (Vo et al., 2012; Bostrom and Mikos, 1997; Chen et al., 2010;  
57 Puppi 2010). The risk of disease transmission from allograft bone can be minimised by  
58 processing or devitalization via freeze-drying or irradiation; however, this may reduce the  
59 osteoinductivity and mechanical strength (White et al., 2013; Hau et al., 2008; Nauth et al.,  
60 2011). Other options include the usage of bone morphogenetic proteins (BMPs), distraction  
61 osteogenesis and bone cement; however, these are also not ideal (Amini et al., 2013). The  
62 shortcomings in the current clinical options have led to concerted efforts in search of  
63 alternative strategies for the repair of bone.

64 Poly (DL-lactic-co-glycolic acid) (PLGA) is a well-studied synthetic polymer used in  
65 bone tissue engineering. It has favourable properties such as biodegradability (Pan and Ding,

66 2012), cytocompatibility, controllable mechanical properties (Bostrom and Mikos, 1997;  
67 Burg et al., 2000; Chen et al., 2010; Puppi et al., 2010) and it can be easily processed (Burg et  
68 al., 2000; Pan and Ding, 2012). Furthermore, PLGA has been approved by the FDA for use in  
69 certain clinical applications (Lu et al., 2009).

70 The combination of porous and non-porous microspheres, which are able to sinter at  
71 body temperature, enables the introduction of porosity within injected scaffolds, hence,  
72 allowing proliferating cells access to nutrients [Qutachi et al., 2014; Boukari et al., 2015].  
73 Simultaneously, the delivery of growth factors such as BMPs to the growing cells is also  
74 facilitated. BMPs have been studied for their use in non-union bone defects, spinal fusion and  
75 open tibial fractures (Boukari et al., 2015; Whilte et al., 2013; Hau and Wang, 2008).  
76 Furthermore, it has been reported that one such BMP, BMP-2, is present during the initial  
77 phase of fracture repair, and during chondrogenesis and osteogenesis (Patel et al., 2008).

78 Various strategies have been utilized for the sintering of microspheres into scaffolds.  
79 These include the incorporation of plasticizers in order to reduce polymer glass transition  
80 temperatures (Dhillon et al., 2011), the addition of organic solvents such as dichloromethane  
81 (Pan and Ding, 2012; Wang et al., 2010) and the application of heat (Delloye et al., 2007;  
82 Chen et al., 2010; Puppi et al, 2010). Although the use of high temperatures and organic  
83 solvents result in mechanically strong scaffolds, these conditions are not ideal for the body  
84 and so are not suitable for sintering *in-situ*. Therefore, a system capable of sintering at 37°C  
85 *in situ* would be extremely beneficial.

86 Protein-loaded PLGA microspheres often exhibit an initial burst release (Boukari et al.,  
87 2015; Tao et al., 2014) which is not ideal for an intended controlled release of BMP-2 at a  
88 defect site. A number of strategies have been employed to control the release of proteins from  
89 PLGA microspheres. These include varying the polymer molecular weight (Boukari et al.,

90 2015), the inclusion of additives such as poloxamer 188 (Paillard-Giteau et al., 2010) and the  
91 use of a PLGA-PEG-PLGA triblock polymer (White et al., 2013; Kirby et al., 2011).

92 Chitosan is a natural polysaccharide derived from chitin and is popular in tissue  
93 engineering applications for a variety of reasons, which include its cytocompatibility and  
94 ability to promote cell adhesion (Amini et al., 2012). Chitosan microspheres show promise  
95 for use in the encapsulation of proteins and have previously been shown to retain the activity  
96 of a neural growth factor (Zeng et al., 2011). Moreover, due to its cationic nature and  
97 propensity to slow degradation, chitosan-based materials are able to sustain the release of  
98 growth factors (Qian and Zhang, 2013). Chitosan has been used in combination with PLGA  
99 in various forms, including by embedding PLGA microspheres into chitosan scaffolds (Kirby  
100 et al., 2011; Zeng et al., 2011; Di Martino et al., 2005; Qian, 2013). PLGA/chitosan  
101 microspheres can be formulated in a variety of ways. These include the use of supercritical  
102 fluid technology (Cassetari et al., 2011), the double emulsion method (Fu et al., 2012; Hu et  
103 al., 2008) the solvent evaporation technique (Jian et al., 2010), an electro-dropping layer-by-  
104 layer approach (Choi et al., 2013) and conjugation and adsorption methods (Chakravarthi and  
105 Robinson, 2011). Porous microspheres have also been treated with chitosan (Yue et al., 2015)  
106 (Chakravarthi and Robinson, 2011), whilst others have encapsulated protein-loaded chitosan  
107 microspheres into large porous PLGA microspheres (Tao et al., 2014).

108 In a previous study, we reported the formulation of a novel PLGA scaffold delivery  
109 system based on porous and protein-loaded microspheres that sintered at 37°C (Boukari et al.,  
110 2015). There have been a number of reports utilising composites of PLGA/chitosan  
111 microspheres for use in bone tissue engineering (Casettari et al., 2011; Han et al., 2015;  
112 Pandey et al., 2013; Jiang et al., 2010; Choi et al., 2013; Chakravarthi and Robinson, 2011).  
113 In the present work, we report the development of a ‘dual-application’ PLGA/chitosan  
114 composite scaffold formulation which sinters at 37°C when injected through a hypodermic

115 needle as well as when implanted as a paste. Furthermore, we aimed to control the release  
116 kinetics of a model protein for BMP-2 (BMP-2 itself was not used due to the cost  
117 implications) from this system, via the inclusion of chitosan, and to investigate its  
118 cytocompatibility and osteoinductive capabilities on primary human mesenchymal stem cells  
119 (hMSCs).

## 120 **2. Materials and methods**

### 121 **2.1 Materials**

122 PLGA (85:15, 53 kDa) was purchased from Evonik (Morris, NJ, USA). Chitosan, low  
123 molecular weight,  $\geq 75\%$  deacetylation; sodium tripolyphosphate (TPP); poly vinyl alcohol  
124 (PVA), 87–89% hydrolysed; phosphate buffered saline (PBS; 0.01 M phosphate buffer,  
125 0.0027 M potassium chloride and 0.137 M sodium chloride; pH 7.4) tablets; sodium  
126 hydroxide (NaOH) pellets; Triton X-100; goat serum; Hoechst 33258; sodium thiosulphate  
127 solution; silver nitrate solution; formalin 10% v/v and paraformaldehyde 10% v/v solutions  
128 were purchased from Sigma-Aldrich (St. Louis, MO, USA). Glacial acetic acid was  
129 purchased from R&M Chemicals (Essex, UK). Dichloromethane (DCM), dimethyl sulfoxide  
130 (DMSO) and sodium dodecyl sulphate (SDS) were purchased from Fisher Scientific UK  
131 (Loughborough, UK). Bovine serum albumin (BSA) was purchased from Nacalai Tesque  
132 (Kyoto, Japan). A micro BCA protein assay kit was purchased from Thermo Fisher Scientific  
133 (Waltham, MA, USA). For stem cell culture, hMSCs, an MSCGM hMSC SingleQuot kit,  
134 trypsin/EDTA for MSC and HEPES buffered saline were purchased from Lonza (Basel,  
135 Switzerland). Presto Blue cell viability reagent was purchased from Gibco, Life Technologies  
136 (Carlsbad, CA, USA). For immunostaining, anti-osteocalcin polyclonal antibody was

137 purchased from Merck Millipore (Billerica, MA, USA) and alexa flour 488 goat anti-rabbit  
138 IgG was purchased from Invitrogen (Carlsbad, CA, USA).

## 139 **2.2 Formulation of PLGA microspheres**

140 Porous PLGA microspheres were prepared using the double emulsion solvent  
141 evaporation method as described in detail elsewhere (Qutachi et al., 2014; Boukari et al.,  
142 2015). Briefly, a 250- $\mu$ l aliquot of PBS was added to a 20% w/v PLGA/DCM solution and  
143 homogenized at 9000 rpm using a Silverson L5M homogeniser (East Longmeadow, MA,  
144 USA). This was added to 200 ml of 0.3% w/v PVA solution and homogenized at 4000 rpm  
145 and then stirred at 300 rpm for 4 hours. The microspheres were washed with distilled water  
146 and then exposed to ethanolic-NaOH in order to enhance the surface porosity. They were  
147 then sieved (40  $\mu$ m) and washed using distilled water. Non-porous microspheres were  
148 prepared in a similar way using 100  $\mu$ l of 100 mg/ml BSA solution or 100  $\mu$ l of distilled  
149 water, instead of 250  $\mu$ l of PBS. BSA was chosen as a model protein as it is compatible with  
150 chitosan and has previously been used as a substitute for growth factors (Song et al., 2013;  
151 Yilgor et al., 2010; Yilgor et al.,2009).

152 Non-porous PLGA/chitosan composite microspheres were prepared similarly;  
153 however, instead of using 200 ml of 0.3% w/v PVA solution, the aqueous phase comprised  
154 150 ml of 0.4% w/v PVA solution containing 0.05 g of TPP. The primary emulsion, in  
155 addition to 50 ml of 0.25% w/v chitosan solution in 2% v/v acetic acid, was added to the  
156 external aqueous phase simultaneously and homogenized. All microspheres were freeze-dried  
157 using a Thermo Fisher Scientific FR-Drying Digital Unit (Waltham, MA, USA) for 48 hours  
158 and stored at -20°C until use.

### 159 **2.3 Scanning electron microscopy (SEM) and size analysis**

160 The freeze-dried samples were mounted onto aluminium stubs (Agar Scientific, UK)  
161 and gold-coated using a Balzers SCD030 gold sputter coater (Balzers Union Ltd.,  
162 Lichtenstein). The morphology and surface topography of the microspheres were observed  
163 using a Jeol 6060L SEM imaging system (Jeol Ltd., Hertfordshire, UK) at 10 kV. The  
164 particle size distribution and mean microsphere diameter were determined using a Coulter  
165 LS230 particle size analyser (Beckman, UK).

### 166 **2.4 Fourier transform infrared (FTIR) spectroscopy**

167 FTIR spectra of the microspheres and their constituents were obtained using a  
168 Spectrum RX 1 FTIR spectrophotometer (Perkin Elmer, **Waltham, MA**, USA). Samples were  
169 mixed with potassium bromide (KBr) and compressed using a 5-tonne force into disks; 256  
170 scans were acquired from 400 to 4000  $\text{cm}^{-1}$ .

### 171 **2.5 Preparation of 3D scaffolds**

172 PLGA and PLGA/chitosan composite scaffolds were previously prepared in our  
173 laboratories (Boukari et al., 2015). A 1:1 mass ratio of porous to non-porous microspheres  
174 was mixed in a weighing boat followed by mixing with PBS (pH 7.4) at a ratio of 0.25:1  
175 (PBS to microspheres) to form a paste. The paste was packed into a 6-mm diameter and 12-  
176 mm height polytetrafluorethylene (PTFE) mould using a spatula, and then stored in a sealed  
177 de-humidifying chamber at 37°C for 17 hours.

178

### 179 **2.6 Time of flight secondary ion mass spectrometry (ToF-SIMS)**

180 The presence and distribution of the chitosan coating on the scaffold surfaces was  
181 assessed using a time of flight secondary ion mass spectrometer (ToF-SIMS IV, ION-TOF  
182 GmbH, Munster, Germany). Scaffolds were placed on the ToF-SIMS stage and secured with  
183 metal clips. A 25-keV Bi<sub>3</sub><sup>+</sup> primary ion source was used to scan a 256 × 256 pixel raster,  
184 while simultaneously not exceeding the limit of static, as described by Rafati et al., (2012).  
185 Surface charge due to the primary ion beam on the insulating sample surface was  
186 compensated using a flood gun generating low energy electrons (20 eV). Negative and  
187 positive polarity data for 500 × 500 μm areas were analysed using the SurfaceLab 6 software  
188 (IONTOF, Germany). PLGA was identified by the presence of C<sub>3</sub>H<sub>3</sub>O<sub>2</sub><sup>-</sup> (*m/z* = 71) and  
189 C<sub>3</sub>H<sub>5</sub>O<sub>2</sub><sup>-</sup> (*m/z* = 73) (Rafato et al., 2012). Diagnostic secondary ion peaks for chitosan were  
190 identified as CN<sup>-</sup> (*m/z* = 26) from the negative polarity data, in addition to CH<sub>4</sub>N<sup>+</sup> (*m/z* = 30)  
191 and C<sub>4</sub>H<sub>5</sub>N<sub>2</sub><sup>+</sup> (*m/z* = 81) from the positive polarity data. For a semi-quantitative analysis, each  
192 area was split into four regions of interest, and the ion intensity data for these peaks of  
193 interest were exported and normalized to the total ion intensity.

## 194 **2.7 Encapsulation efficiency (%EE) of BSA within microspheres and scaffolds**

195 The %EE of BSA within the non-porous PLGA and PLGA/chitosan composite  
196 microspheres and scaffolds were determined by gently stirring 10 mg of the microspheres or  
197 one scaffold in 750 μl or 13 ml of DMSO, respectively, for 1 hour. This was followed by the  
198 addition of 2.15 ml or 37.27 ml of 0.02% w/v SDS in 0.2 M NaOH to the microspheres or  
199 scaffolds, respectively. The solution was left to stand at room temperature for 1 hour.  
200 Standard concentrations of BSA were calibrated with a BCA reagent so that the sample  
201 absorbance could be matched with standard concentrations on an Infinite 200 plate reader  
202 (Tecan, Switzerland) at 562 nm. The %EE of BSA within the microspheres and scaffolds was  
203 then calculated using Equation 1.

204 
$$\%EE = \frac{\text{Actual mass of BSA in 10mg of microspheres OR 1 scaffold}}{\text{Theoretical mass of BSA used for 10 mg of microspheres OR 1 scaffold}} \times 100 \quad (1)$$

205

## 206 **2.8 Release of BSA from microspheres and scaffolds**

207 Release studies of BSA from the PLGA and PLGA/chitosan composite microspheres  
208 were carried out by submerging 50 mg of microspheres in 1.5 ml of PBS in a micro-  
209 centrifuge tube. The tubes were incubated at 37°C. At predetermined time intervals, the PBS  
210 supernatant was removed and replaced with fresh buffer. Aliquots (150 µl) were withdrawn  
211 from the supernatant and assayed for the presence of BSA at 562 nm on the microplate reader  
212 using the BCA assay kit. BSA release from scaffolds was studied in 4 ml of PBS and assayed  
213 as described above.

214

## 215 **2.9 Preparation of 3D scaffolds post-injection**

216 Microsphere mixtures were prepared at a 1:1 ratio of porous to non-porous  
217 microspheres and an approximate BSA loading of 3 mg of BSA/g of mixture, as described in  
218 section 2.5. The mixture was suspended in PBS at a concentration of 50 mg of  
219 microspheres/ml, vortex-mixed briefly and then drawn into a 1-ml syringe (BD Fine) fitted  
220 with a 19-G needle (1.1 × 50 mm, BD fine, Franklin Lakes, NJ, USA). Finally, the contents  
221 of the syringe were injected into the PTFE scaffold mould.

222

## 223 **2.10 Compressive strength of scaffolds**

224 The compressive strength of the scaffolds was assessed using a TA.HD+ texture  
225 analyser (Stable Microsystems, UK) equipped with a 50-kg load cell at a speed of 0.04

226 mm/second over a contact area of approximately 28.75 mm<sup>2</sup>. Dry PLGA and PLGA/chitosan  
227 BSA-loaded scaffolds prepared as described in sections 2.5 and 2.9 were tested, and the  
228 compressive strength was determined as the stress at the maximum strain.

229

## 230 **2.11 Cell culture and seeding onto scaffolds**

231 Primary hMSCs were cultured in hMSC basal media supplemented with the contents  
232 of an MSCGM hMSC SingleQuote kit. The cells were maintained in a humidified tissue-  
233 culture incubator at 37°C in 5% CO<sub>2</sub>. The cytocompatibility test was carried out on BSA-free  
234 scaffolds. Scaffolds were prepared directly into a 24-well plate in a manner similar to that  
235 described in section 2.5. A 1:1 porous to non-porous microsphere mixture was UV sterilised  
236 for 80 minutes (Gould et al., 2013) and then transferred to the well. Basal growth medium  
237 was then added at a ratio of 0.25:1 (medium to microspheres). After 17 hours of sintering,  
238 each scaffold was seeded with  $1 \times 10^5$  hMSCs and incubated for 2 hours, followed by the  
239 addition of 1 ml of media to each scaffold/well. The cell-seeded scaffolds were maintained at  
240 37°C with 5% CO<sub>2</sub>. For all cell experiments, either 5 replicates or 2 independent repeats each  
241 comprising at least 3 replicates was carried out.

## 242 **2.12 Cell viability assay**

243 Each scaffold was submerged in 1 ml of media and 111 µl of Presto Blue reagent and  
244 the cell viability was determined at day 1, 3, 6 and 8 post-seeding using the Presto Blue cell  
245 viability reagent. The well plate was protected from light and incubated at 37°C for 25  
246 minutes. Aliquots of 100 µl were withdrawn from each well in triplicate and the absorbance  
247 was read on an infinite 200 plate reader (Tecan, Switzerland) at excitation and emission  
248 wavelengths of 560 nm and 590 nm, respectively. The Presto Blue reagent was replaced with

249 fresh media and the scaffolds were placed back in the incubator. On day 8, after measuring  
250 the cell viability, the scaffolds were washed with PBS and the cells were fixed with 10% v/v  
251 buffered formalin solution for 20 minutes. Fixed hMSC-scaffold constructs were viewed  
252 under the SEM.

### 253 **2.13 Assessment of mineralization**

254 In order to determine the degree of mineralization on the scaffolds, the von Kossa  
255 assay was utilized. Cells were seeded onto scaffolds as described in section 2.11 and  
256 incubated in basal growth media for 21 days. On day 21, cells were fixed with 10% v/v  
257 buffered formalin for 20 minutes and thoroughly washed with PBS. A 450- $\mu$ l aliquot of 1%  
258 w/v silver nitrate solution was added to each scaffold and incubated under a UV light source  
259 for 1 hour. The solution was then removed and the scaffolds were washed three times with  
260 deionized water. This was followed by treatment with sodium thiosulphate solution for 5  
261 minutes in order to remove any excess silver nitrate solution. The scaffolds were then washed  
262 with PBS prior to imaging under a dissection microscope (Leica, Germany).

263

### 264 **2.14 Osteocalcin immunostaining**

265 Cells were seeded onto scaffolds as described in section 2.11. The scaffolds were  
266 incubated in basal growth media for 21 days after which they were fixed using 10% v/v  
267 paraformaldehyde for 20 minutes and then thoroughly washed with PBS. The cells were  
268 permeabilised with 500  $\mu$ l of 0.1% v/v Triton X-100 solution for 40 minutes. The solution  
269 was aspirated and the cells were washed with PBS. Blocking of unspecific binding sites as a  
270 result of epitomes on the cell layers was carried out via the addition of 500  $\mu$ l of 3% v/v goat  
271 serum in 1% w/v BSA in PBS for 40 minutes. The blocking solution was removed and 500  $\mu$ l

272 of anti-OCN primary antibody solution (1:200 dilution in 1% w/v BSA in PBS) was added.  
273 The scaffolds were incubated at 4°C overnight. After incubation, the antibody solution was  
274 removed, the scaffolds were washed with PBS and then incubated at room temperature for  
275 two hours in 500 µl of a 1:200 solution of Alexa Fluor 488 goat anti-rabbit secondary IgG, in  
276 1% w/v BSA in PBS. After incubation, the secondary antibody solution was removed and the  
277 scaffolds were washed with PBS. In order to stain the DNA of cells, the scaffolds were  
278 incubated for a further 15 minutes in 1 µg/ml Hoechst dye dissolved in 1% w/v BSA in PBS  
279 at room temperature. After incubation, the Hoechst dye was removed and the scaffolds were  
280 thoroughly washed with PBS and then viewed under a dissection microscope. The images of  
281 PLGA and composite scaffolds were processed and compared using the ImageJ software  
282 (Version 1.48, National Institute of Health, Bethesda, MD, USA). Four images were taken of  
283 four different areas on each scaffold and then converted into binary formats so that the  
284 stained areas could be calculated.

285

## 286 **2.15 Statistical Analyses**

287 A statistical analysis of the data was carried out using Microsoft Excel. An unpaired t test and  
288 the ANOVA procedure were used and the results were deemed significant when  $p < 0.05$ .

## 289 **3. Results**

### 290 **3.1 Physical characterization of PLGA/chitosan composite microspheres and scaffolds**

291 BSA-encapsulated PLGA/chitosan composite microspheres were formulated using  
292 TPP as a cross-linker as detailed in section 2.2. Both the PLGA and composite microspheres  
293 appeared smooth, as shown in the SEM images in Figure 1A and B, respectively. Thus, the

294 addition of chitosan cross-linked with TPP did not alter the superficial appearance of the  
295 microspheres and no unprocessed, free chitosan is visible from the SEM images. Size  
296 analysis revealed the average diameters of the PLGA and composite microspheres to be  $69.75$   
297  $\pm 21.47 \mu\text{m}$  and  $66.85 \pm 22.68 \mu\text{m}$ , respectively (Figure 1C).

298  
299 The FTIR spectra of the raw materials and microspheres are presented in Figure 2.

300 The chitosan spectrum shows a high-intensity peak at  $3400 \text{ cm}^{-1}$ , which corresponds to  
301 stretching vibrations of the O-H and N-H bonds, in addition to hydrogen bonding in the  
302 backbone (Azevedo et al., 2011). The characteristic peak at  $1647 \text{ cm}^{-1}$  is a result of the amide  
303 functionality and may be present as a consequence of the axial deformation of the C=O bond  
304 (Azevedo et al., 2011) and strong N-H bending (Misch et al., 1999). Peaks present at  $1019$   
305 and  $1086 \text{ cm}^{-1}$  (corresponding to C-O stretch vibrations), and  $1152 \text{ cm}^{-1}$  (asymmetric stretch  
306 of the C-O-C bond) are also indicative of chitosan (Azevedo et al., 2011).

307 The TPP spectrum, similarly, shows a peak of significant intensity at  $3390 \text{ cm}^{-1}$ ,  
308 corresponding to the stretching vibrations of the O-H bond. Peaks around the  $1095 \text{ cm}^{-1}$   
309 region are an indication of the P=O phosphate group. The PLGA spectrum presents a peak at  
310  $3473 \text{ cm}^{-1}$ , which is indicative of vibration of the terminal O-H groups. Other peaks that  
311 indicate PLGA are present at  $743 \text{ cm}^{-1}$  (C-H bend),  $1086$  and  $1180 \text{ cm}^{-1}$  (C-O stretch),  $1381$   
312  $\text{cm}^{-1}$  (C-H bend),  $1771 \text{ cm}^{-1}$  (the carbonyl C=O) and  $2876 \text{ cm}^{-1}$  ( $\text{CH}_2$  bend) (Ganji and  
313 Abdekhodaie, 2010). Both PLGA and PLGA/chitosan composite BSA-loaded microspheres  
314 show peaks at identical wavelengths, which suggests that the microspheres are predominantly  
315 PLGA. Moreover, the spectra of PLGA and PLGA/chitosan composite microspheres show  
316 peaks at  $1621 \text{ cm}^{-1}$  and  $1639 \text{ cm}^{-1}$ , respectively, which are attributed to the C=O bond of the  
317 amide groups that are found both in BSA and chitosan. However, there does appear to be a  
318 slightly more pronounced peak at  $1639 \text{ cm}^{-1}$  on the spectrum of the PLGA/chitosan

319 composite microspheres, which corresponds to the amide C=O bond suggesting the presence  
320 of chitosan in the formulation.

321 The ToF-SIMS analysis was carried out in order to ascertain the presence of chitosan  
322 on the scaffold surfaces. BSA-free scaffolds were analysed based on the overlap of chitosan  
323 and BSA secondary ion peaks (discussed in section 2.6). Intensities of nitrogen-containing  
324 positive secondary ion peaks  $\text{CH}_4\text{N}^+$  ( $m/z = 30$ ) and  $\text{C}_4\text{H}_5\text{N}_2^+$  ( $m/z = 81$ ), as well as the  
325 negative ion peak  $\text{CN}^-$  ( $m/z = 26$ ) were all significantly higher in the composite  
326 PLGA/chitosan scaffolds when compared to the chitosan-free scaffolds, as shown in Figure  
327 3A. However, there was no significant difference between the profiles of diagnostic PLGA  
328 ion peaks for the PLGA and composite scaffolds (Figure 3B).

329 The incorporation of chitosan did not elicit a significant change in the encapsulation  
330 efficiency of BSA in the microspheres, with  $80.58 \pm 17.06\%$  and  $81.57 \pm 3.06\%$  of the  
331 protein being encapsulated into the PLGA and PLGA/chitosan composite microspheres,  
332 respectively. Moreover, there was no statistical difference in the encapsulation efficiencies of  
333 the PLGA and composite scaffolds ( $2.81 \text{ mg/g}$  [ $93.68\% \pm 3.50\%$ ] and  $2.52 \text{ mg/g}$  [ $84.02\% \pm$   
334  $12.08\%$ ] for the PLGA and PLGA/chitosan composite scaffolds, respectively).

### 335 **3.2 Release of BSA from microspheres and scaffolds**

336 The release profile of BSA was mapped over 28 days from both microspheres and  
337 scaffolds sintered at  $37^\circ\text{C}$  (Figure 4). The initial burst release after 24 hours from the PLGA  
338 microspheres was significantly higher than from the PLGA/chitosan composite microspheres,  
339  $0.93 \pm 0.06 \mu\text{g/mg}$  and  $0.57 \pm 0.03 \mu\text{g/mg}$ , respectively ( $p < 0.05$ ). After 28 days,  $1.72 \pm 0.23$   
340  $\mu\text{g/mg}$  of BSA was released from the PLGA microspheres, which was ~~significantly~~ higher in  
341 comparison to  $1.20 \pm 0.05 \mu\text{g/mg}$  from the PLGA/chitosan composite microspheres ( $p = 0.05$ )

342 Similarly, there was a significant retardation of the initial burst release from the  
343 scaffolds containing PLGA/chitosan composite microspheres,  $0.10 \pm 0.02 \mu\text{g}/\text{mg}$ , in  
344 comparison to the PLGA scaffolds,  $0.16 \pm 0.01 \mu\text{g}/\text{mg}$  ( $p < 0.05$ , Figure 4B).

345

### 346 **3.3 Sintering of microspheres into scaffolds**

347 In order to study the effect of the scaffold preparation method on their subsequent  
348 morphology and mechanical strength, the PLGA and PLGA/chitosan composite scaffolds  
349 were prepared using two different methods. Firstly, a paste was formed from the  
350 microspheres as previously reported (Boukari et al., 2015). In the second method, we aimed  
351 to study the ability of the microspheres to sinter post-injection through a 19-G needle into a  
352 scaffold mould. This was then followed by a 17-hour incubation period at  $37^\circ\text{C}$ . Photographs  
353 of the resulting scaffolds and their compressive strengths are presented in Figure 5A and B,  
354 respectively. The sintering process results in the expulsion of water so that the components  
355 within close proximity. We believe that this favours ‘fusion’ and bond formation within the  
356 scaffolds. This approach to scaffold sintering at  $37^\circ\text{C}$  is superior to the more harsh methods  
357 employing elevated temperatures and reagents.

358 The overall appearances of PLGA and composite scaffolds were very similar (Figure  
359 5A). However, when comparing scaffolds prepared using the paste method, the compressive  
360 strength of PLGA/chitosan composite scaffolds was significantly higher ( $0.846 \pm 0.272 \text{ MPa}$ )  
361 than the PLGA scaffolds ( $0.406 \pm 0.265 \text{ MPa}$ ,  $p < 0.05$ ).

362 Figure 5A shows that it was possible to successfully sinter a microsphere suspension  
363 post-injection, thus, forming intact scaffolds **that retained their shape when removed from the**  
364 **mould**. This confirms the injectable potential of the microspheres. When scaffolds were

365 sintered as a suspension post-injection, there was no significant difference between the  
366 compressive strengths of the PLGA and PLGA/chitosan composite scaffolds,  $0.086 \pm 0.068$   
367 MPa and  $0.048 \pm 0.00096$  MPa, respectively ( $p > 0.05$ , Figure 5B); however, it is likely that  
368 the compressive values may be below the lower limit of threshold of the machine.

369

### 370 **3.4 Cell proliferation on scaffolds**

371 The culturing of primary hMSCs on the scaffolds was used as a means to test their  
372 cytocompatibility. Cell proliferation was assessed using the Presto Blue viability reagent on  
373 day 1, 3, 6 and 8 (Figure 6A).

374 Cell proliferation increased over time on both scaffold types. On day 1, the cell  
375 numbers on PLGA and PLGA/chitosan composite scaffolds were  $1.06 \times 10^4$  and  $1.03 \times 10^4$ ,  
376 respectively. Both types of scaffolds exhibited a very similar cell growth profile with no  
377 statistically significant difference found between them ( $p > 0.05$ ) on day 1, 3 and 6. However,  
378 the cell number on day 8 was significantly higher on the PLGA scaffolds ( $p < 0.05$ ) at  $6.25 \times$   
379  $10^4$  and  $4.45 \times 10^4$  for PLGA and PLGA/chitosan composite scaffolds, respectively. SEM  
380 images of the cell-scaffold constructs on day 8 are shown in Figure 6B and C, with cells  
381 visibly distributed between microspheres in both scaffold types.

382

### 383 **3.5 Assessment of mineralization**

384 The extent of mineralization on the scaffolds after 21 days in culture media was  
385 assessed using the von Kossa assay as described in section 2.14. Dark brown/black nodules  
386 (indicated by the white arrow in Figure 7B) are visible on the scaffolds and represent positive  
387 staining. A qualitative analysis shows that there are more nodules on the PLGA/chitosan

388 composite scaffolds (Figure 7B), which appear darker in the figure, in comparison to the  
389 PLGA scaffolds (Figure 7A).

### 390 **3.6 Osteocalcin immunostaining**

391 The presence of the bone marker protein, osteocalcin, was detected using the  
392 immunostaining technique described in section 2.14. The data obtained was processed using  
393 ImageJ, which allowed us to quantify the amount of stain present on each scaffold. The  
394 results of this analysis show that there was an increase in osteocalcin staining on the  
395 composite scaffolds when compared to the PLGA scaffolds ( $p < 0.05$ , Figure 8A). When  
396 osteogenic media was used (data not shown), the osteocalcin staining on the PLGA/chitosan  
397 and PLGA scaffolds was not significantly different ( $p > 0.05$ ). Processed, merged images are  
398 shown in Figure 8B and C, with osteocalcin represented in green, and cell DNA in blue.

## 399 **4. Discussion**

400 Scaffolds made from biodegradable microspheres are a promising approach for bone  
401 regeneration. However, there are several features to consider when developing such systems.  
402 These include the incorporation of porosity and growth factors into the scaffolds, whilst at the  
403 same time providing mechanical strength to enable the microspheres to be injectable and  
404 sinter *in situ*. Some research groups have developed scaffolds with some of these properties;  
405 however, most groups do not take into account all desirable features in one system. In the  
406 present study, we propose a novel dual-application PLGA/chitosan composite scaffold  
407 system with the potential to meet all of the above desirable criteria. The system comprises  
408 porous and non-porous protein-loaded microspheres with the ability to sinter at 37°C and  
409 release protein. The mechanical strength of the system is dependent upon its mode of  
410 application, with a higher compressive strength achievable when it is applied as a paste, and  
411 sufficient strength to maintain the shape (as evident from the fact that the microspheres

412 sintered at 37°C and were subsequently removed from the mould intact) when injected as a  
413 suspension. The cytocompatibility and osteogenic potential of the formulation were  
414 evaluated and compared with our previously reported system (Boukari et al., 2015).

415 Protein-loaded microspheres were formulated using PLGA and chitosan, where the  
416 chitosan was cross-linked using TPP. There were no observable differences in the  
417 morphology and size of the composite microspheres when compared with PLGA  
418 microspheres. The presence of chitosan within the composite scaffolds formed via the paste  
419 method was confirmed by ToF-SIMS, suggests that chitosan is formed as part of the  
420 microstructure of the particles. Furthermore, the composite scaffolds demonstrated higher  
421 compressive strength than the PLGA scaffolds. In this regard, chitosan contributes to the  
422 mechanical strength of the scaffolds, due to interactions between the negatively charged  
423 PLGA (Balmert et al., 2015) and the protonated amine groups in the chitosan structure.  
424 Moreover, the compressive strength demonstrated by the composite scaffolds fell within an  
425 acceptable range as reported by Misch et al. (1999).

426 The chitosan coating attenuated the initial burst release from the microspheres and  
427 scaffolds, and this reduction may partly be attributed to chitosan complexing with BSA  
428 (isoelectric point, approximately 5), thereby, impeding its release. The ability of chitosan, a  
429 natural polyelectrolyte, to non-covalently bind to negatively charged proteins has been  
430 reported (Boeris et al., 2010). A similar observation of a reduced burst release was made for  
431 the same system when encapsulated with lysozyme, which is positively charged at a neutral  
432 pH (data not shown). This suggests that other factors contribute to the reduction in burst  
433 release. It has been reported that the burst release of proteins from PLGA microspheres is  
434 usually due to protein residing near, or on the surface of, the delivery system (Zeng and  
435 Liang, 2010). We believe that the formation of a chitosan -TPP matrix layer slows the release  
436 of the protein and significantly contributes to the attenuation in the initial burst release. This

437 effect has been demonstrated in PLGA/chitosan microspheres encapsulated with a non-  
438 protein drug, rifampicin, in which the addition of chitosan caused a reduction in the burst  
439 release (Manca et al., 2008). The slower, steadier release of BSA from the microspheres and  
440 scaffolds containing PLGA/chitosan is desirable in BMP-2 applications. The controlled  
441 release reduces the need for supra-physiological loadings, which are necessary when there is  
442 a huge initial loss via a burst release (Kirby et al., 2011).

443         The system described herein possesses dual-applicability arising from the  
444 formulation's potential of having two application modes (i) a paste that is implanted within a  
445 degenerated bone tissue, takes the shape of the defect area and then sinters at 37°C, and (ii)  
446 the injection of the microsphere suspension directly into the defect area. The former would be  
447 useful in applications requiring a relatively stronger scaffold, such as the regeneration of  
448 cancellous bone for which the ultimate compressive strength has been reported to range from  
449 0.22 to 10.44 MPa (Misch et al., 1999). However, the latter is more suited to applications in  
450 which the delivery system may be injected and remain in one location, hence, allowing the  
451 controlled delivery of a specific, known dose of protein to the site. To our knowledge, this is  
452 the first time that the ability of microspheres to sinter at 37°C, post-injection, has been  
453 demonstrated.

454         The ability of cells to attach and grow on the scaffolds is paramount in the  
455 development of protein delivery systems in regenerative medicine. For this reason, the  
456 cytocompatibility of the scaffolds with hMSCs was investigated. The cell number increased  
457 on the composite scaffolds over the 8-day period from  $1.03 \times 10^4$  on day 1, to  $4.45 \times 10^4$  on  
458 day 8. There was no significant difference between cell numbers on the composite and PLGA  
459 scaffolds, except on day 8, by which time the cell numbers were higher on PLGA scaffolds ( $p$   
460  $< 0.05$ ). Although previous studies have investigated the cytocompatibility of sintered

461 composite PLGA/chitosan microspheres scaffolds with other cell types, these formulations  
462 were not capable of sintering *in situ* (Tao et al., 2014).

463 The potential of the scaffold material to promote the differentiation of hMSCs is  
464 another key factor that is crucial for the production of a successful biomaterial. Although the  
465 presence of BMP-2 has been shown to promote osteogenic differentiation, the intrinsic ability  
466 of the material itself to promote the process is also of interest. Chitosan has been reported to  
467 have numerous biomedical properties, including its ability to improve osteogenesis in animal  
468 bone defect models (Lee et al., 2008). In this study, we investigated the cell response to  
469 protein-free scaffolds in basal media in order to study the effect of the scaffold material on  
470 osteogenesis. The presence of a calcified ECM is a reliable way of confirming osteogenesis  
471 (Declercq et al., 2005). Nodules were observed on both composite and PLGA scaffolds based  
472 on von Kossa staining, which indicates the presence of calcium. To provide further  
473 confirmation of the deposition of a calcified matrix, the presence of osteocalcin, a late protein  
474 marker of osteogenic differentiation, was determined. Its expression is known to rise with an  
475 increase in mineralization (Stein et al., (1990). The composite scaffolds showed a  
476 significantly higher degree of osteocalcin staining when compared to the PLGA scaffolds.  
477 Previous studies have demonstrated the ability of chitosan-containing scaffolds to induce  
478 differentiation in the presence of osteogenic media (Jiang et al., 2006), which we also  
479 confirmed (data not shown). However, relatively little evidence has demonstrated this in  
480 basal growth media. Therefore, these results suggest that the inclusion of chitosan in PLGA  
481 microspheres enhanced the osteogenic capacity of the resultant scaffolds.

## 482 **5. Conclusion**

483 In this study, a novel, dual-application composite microsphere system was developed  
484 with the ability to fuse together as a paste, thereby forming an intact scaffold in the body at

485 37°C. Furthermore, the ability of a suspension of the microspheres to sinter post-injection  
486 was also demonstrated. Composite PLGA/chitosan microspheres were shown to attenuate the  
487 initial burst release and elicited a steady, slow release of protein over 28 days. The scaffold's  
488 cytocompatibility and ability to promote osteogenesis were also demonstrated. This  
489 technology, therefore, exhibits potential as a scaffold for bone regeneration and is an  
490 excellent candidate for further *in vitro* and *in vivo* testing.

491

#### 492 **Disclosures**

493 There are no potential conflicts of interest to disclose for this work.

#### 494 **Acknowledgements**

495 This work was funded by the European Community under the FP7 project 519  
496 Biodesign EUFP7-NMP.20102.3-1. The authors would also like to thank Enas Alkhader,  
497 Hilda Amekyeh, Abdulrahman Baki and Noura Alom (The University of Nottingham) for  
498 their support and assistance.

499 This article contains supplementary material available from the authors upon request or via  
500 the Internet at <http://wileylibrary.com>.

501

502

503

504

#### 505 **References:**

- 506 Amini AR, Laurencin CT, Nukavarapu SP 2012. Bone Tissue Engineering: Recent Advances  
507 and Challenges. *Crit Rev Biomed Eng* 40: 363–408.
- 508 Azevedo JR, Sizilio RH, Brito MB, Costa a. MB, Serafini MR, Araújo a. a S, et al. 2011.  
509 Physical and chemical characterization insulin-loaded chitosan-TPP nanoparticles. *J Therm*  
510 *Anal Calorim* 106: 685–689.
- 511 Balmert SC, Zmolek AC, Glowacki AJ, Knab TD, Rothstein SN, Wokpetah JM, et al. 2015.  
512 Positive charge of “sticky” peptides and proteins impedes release from negatively charged  
513 PLGA matrices. *J Mater Chem B* 3: 4723–4734.
- 514 Boeris V, Farruggia B, Pico G 2010. Chitosan-bovine serum albumin complex formation: A  
515 model to design an enzyme isolation method by polyelectrolyte precipitation. *J Chromatogr*  
516 *B-Analytical Technol Biomed Life Sci* 878: 1543–1548.
- 517 Bostrom R, Mikos AG 1997. Tissue Engineering of Bone, in: *Synth. Biodegrad. Polmer*  
518 *Scaffolds*, : pp. 215–234.
- 519 Boukari Y, Scurr DJ, Qutachi O, Morris AP, Doughty SP, Rahman C V, Billa N 2015.  
520 Physicomechanical properties of sintered scaffolds formed from porous and protein-loaded  
521 poly(DL-lactic-co-glycolic acid) microspheres for potential use in bone tissue engineering. *J*  
522 *Biomater Sci Polym Ed* 26: 796–811.
- 523 Burg KJ, Porter S, Kellam JF 2000. Biomaterial developments for bone tissue engineering.  
524 *Biomaterials* 21: 2347–2359.
- 525 Casettari L, Castagnino E, Stolnik S, Lewis A, Howdle SM, Illum L 2011. Surface  
526 characterisation of bioadhesive PLGA/chitosan microparticles produced by supercritical fluid  
527 technology. *Pharm Res* 28: 1668–1682.
- 528 Chakravarthi SS, Robinson DH 2011. Enhanced cellular association of paclitaxel delivered in  
529 chitosan-PLGA particles. *Int J Pharm* 409: 111–120.
- 530 Chen FM, Zhang M, Wu ZF 2010. Toward delivery of multiple growth factors in tissue  
531 engineering. *Biomaterials* 31: 6279–6308.
- 532 Choi DH, Subbiah R, Kim IH, Han DK, Park K 2013. Dual growth factor delivery using  
533 biocompatible core-shell microcapsules for angiogenesis. *Small* 9: 3468–3476.
- 534 Declercq H, Verbeeck R, Deridder L, Schacht E, Cornelissen M 2005. Calcification as an  
535 indicator of osteoinductive capacity of biomaterials in osteoblastic cell cultures. *Biomaterials*  
536 26: 4964–4974.
- 537 Delloye C, Cornu O, Druetz V, Barbier O 2007. Bone allografts: What they can offer and  
538 what they cannot. *J Bone Joint Surg Br* 89: 574–579.

- 539 Dhillon A, Schneider P, Kuhn G, Reinwald Y, White LJ, Levchuk A, et al. 2011. Analysis of  
540 sintered polymer scaffolds using concomitant synchrotron computed tomography and in situ  
541 mechanical testing. *J Mater Sci Mater Med* 22: 2599–2605.
- 542 Di Martino A, Sittinger M, Risbud M V. 2005. Chitosan: A versatile biopolymer for  
543 orthopaedic tissue-engineering. *Biomaterials* 26: 5983–5990.
- 544 Fu Y, Du L, Wang Q, Liao W, Jin Y, Dong A, et al. 2012. In vitro sustained release of  
545 recombinant human bone morphogenetic protein-2 microspheres embedded in  
546 thermosensitive hydrogels. *Pharmazie* 67: 299–303.
- 547 Ganji F, Abdekhodaie MJ 2010. Chitosan-g-PLGA copolymer as a thermosensitive  
548 membrane. *Carbohydr Polym* 80: 740–746.
- 549 Gould TW a, Birchall JP, Mallick AS, Alliston T, Lustig LR, Shakesheff KM, Rahman C V  
550 2013. Development of a porous poly(DL-lactic acid-co-glycolic acid)-based scaffold for  
551 mastoid air-cell regeneration. *Laryngoscope* 123: 3156–3161.
- 552 Han F, Zhou F, Yang X, Zhao J, Zhao Y, Yuan X 2015. Facile Preparation of PLGA  
553 Microspheres With Diverse Internal Structure by Modified Double-Emulsion Method for  
554 Controlled Release. *Polym Eng Sci* 55: 896–906.
- 555 Hsu WK, Wang JC 2008. Contemporary concepts in spine care- the use of bone  
556 morphogenetic protein in spine fusion. *Spine J* 8: 419–425.
- 557 Hu X, Zhou J, Zhang N, Tan H, Gao C 2008. Preparation and properties of an injectable  
558 scaffold of poly(lactic-co-glycolic acid) microparticles/chitosan hydrogel. *J Mech Behav*  
559 *Biomed Mater* 1: 352–359.
- 560 Jaklenec A, Hinckfuss A, Bilgen B, Ciombor DM, Aaron R, Mathiowitz E 2008. Sequential  
561 release of bioactive IGF-I and TGF- $\beta$ 1 from PLGA microsphere-based scaffolds.  
562 *Biomaterials* 29: 1518–1525.
- 563 Jaklenec A, Wan E, Murray ME, Mathiowitz E 2008. Novel scaffolds fabricated from  
564 protein-loaded microspheres for tissue engineering. *Biomaterials* 29: 185–192.
- 565 Jiang T, Abdel-Fattah WI, Laurencin CT 2006. In vitro evaluation of chitosan/poly(lactic  
566 acid-glycolic acid) sintered microsphere scaffolds for bone tissue engineering. *Biomaterials*  
567 27: 4894–4903.
- 568 Jiang T, Khan Y, Nair LS, Abdel-Fattah WI, Laurencin CT 2010. Functionalization of  
569 chitosan/poly(lactic acid-glycolic acid) sintered microsphere scaffolds via surface  
570 heparinization for bone tissue engineering. *J Biomed Mater Res A* 93: 1193–1208.
- 571 Jiang T, Nukavarapu SP, Deng M, Jabbarzadeh E, Kofron MD, Doty SB, et al. 2010.  
572 Chitosan-poly(lactide-co-glycolide) microsphere-based scaffolds for bone tissue engineering:  
573 In vitro degradation and in vivo bone regeneration studies. *Acta Biomater* 6: 3457–3470.

574 Kirby GTS, White LJ, Rahman C V., Cox HC, Qutachi O, Rose FRAJ, et al. 2011. PLGA-  
575 Based Microparticles for the Sustained Release of BMP-2. *Polymers (Basel)* 3: 571–586.

576 Lee J-Y, Nam S-H, Im S-Y, Park Y-J, Lee Y-M, Seol Y-J, et al. 2002. Enhanced bone  
577 formation by controlled growth factor delivery from chitosan-based biomaterials. *J Control*  
578 *Release* 78: 187–197.

579 Lu JM, Wang X, Marin-Muller C, Wang H, Lin PH, Yao Q, Chen C 2009. Current advances  
580 in research and clinical applications of PLGA based nanotechnology. *Expert Rev Mol Diagn*  
581 9: 325–341.

582 Luciani A, Coccoli V, Orsi S, Ambrosio L, Netti P a. 2008. PCL microspheres based  
583 functional scaffolds by bottom-up approach with predefined microstructural properties and  
584 release profiles. *Biomaterials* 29: 4800–4807.

585 Makadia HK, Siegel SJ 2011. Poly Lactic-co-Glycolic Acid (PLGA) as Biodegradable  
586 Controlled Drug Delivery Carrier. *Polymers (Basel)* 3: 1377–1397.

587 Manca ML, Loy G, Zaru M, Fadda AM, Antimisiaris SG 2008. Release of rifampicin from  
588 chitosan, PLGA and chitosan-coated PLGA microparticles. *Colloids Surf B Biointerfaces* 67:  
589 166–70.

590 Martino S, D’Angelo F, Armentano I, Kenny JM, Orlacchio A 2012. Stem cell-biomaterial  
591 interactions for regenerative medicine. *Biotechnol Adv* 30: 338–351.

592 Misch E, Qu Z, Bidez MW 1999. Mechanical properties of trabecular bone in the human  
593 mandible: implications for dental implant treatment planning and surgical placement. *J Oral*  
594 *Maxillofac Surg* 57: 700–706.

595 Nauth A, Ristevski B, Li R, Schemitsch EH 2011. Growth factors and bone regeneration:  
596 how much bone can we expect? *Injury* 42: 574–579.

597 Paillard-Giteau A, Tran VT, Thomas O, Garric X, Coudane J, Marchal S, et al. 2010. Effect  
598 of various additives and polymers on lysozyme release from PLGA microspheres prepared by  
599 an s/o/w emulsion technique. *Eur J Pharm Biopharm* 75: 128–136.

600 Pan Z, Ding J 2012. Poly(lactide-co-glycolide) porous scaffolds for tissue engineering and  
601 regenerative medicine. *Interface Focus* 2: 366–377.

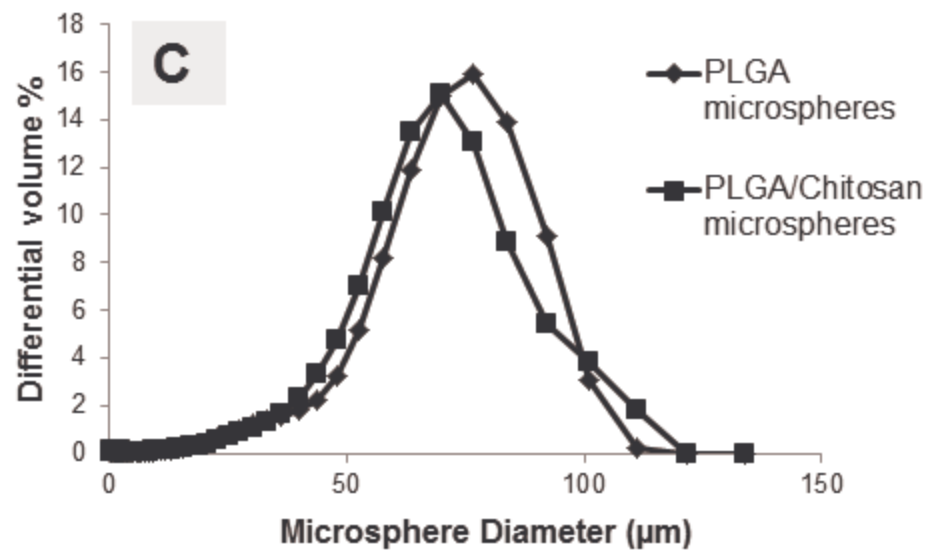
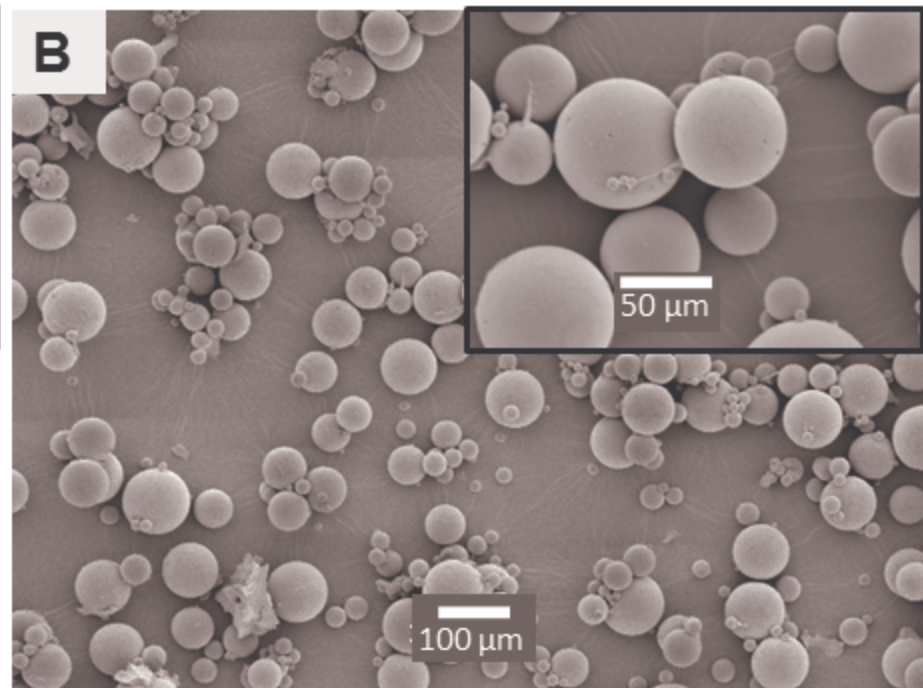
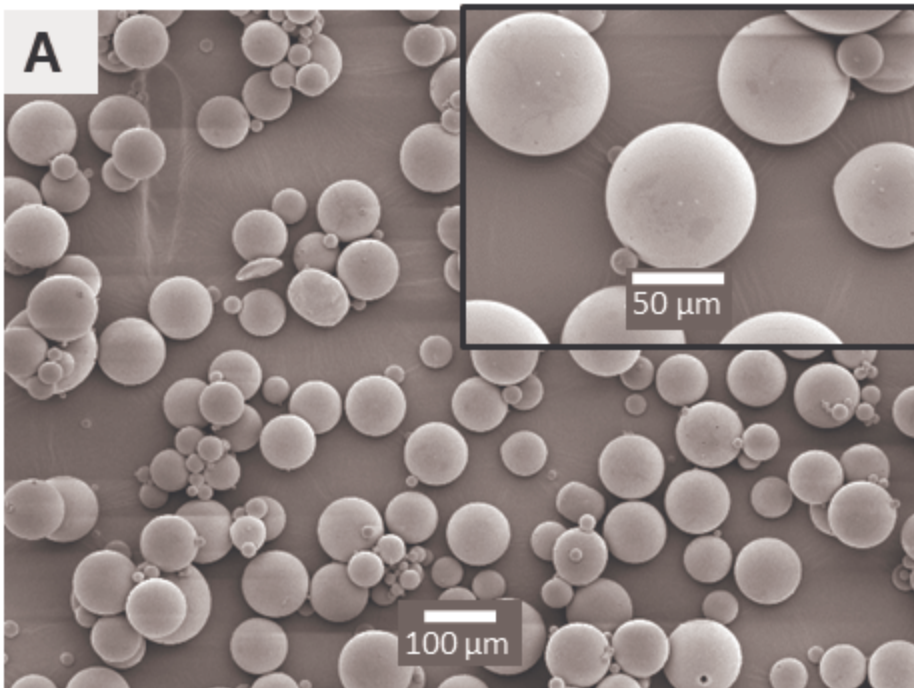
602 Pan Z, Ding J 2012. Poly(lactide-co-glycolide) porous scaffolds for tissue engineering and  
603 regenerative medicine. *Interface Focus* 2: 366–377.

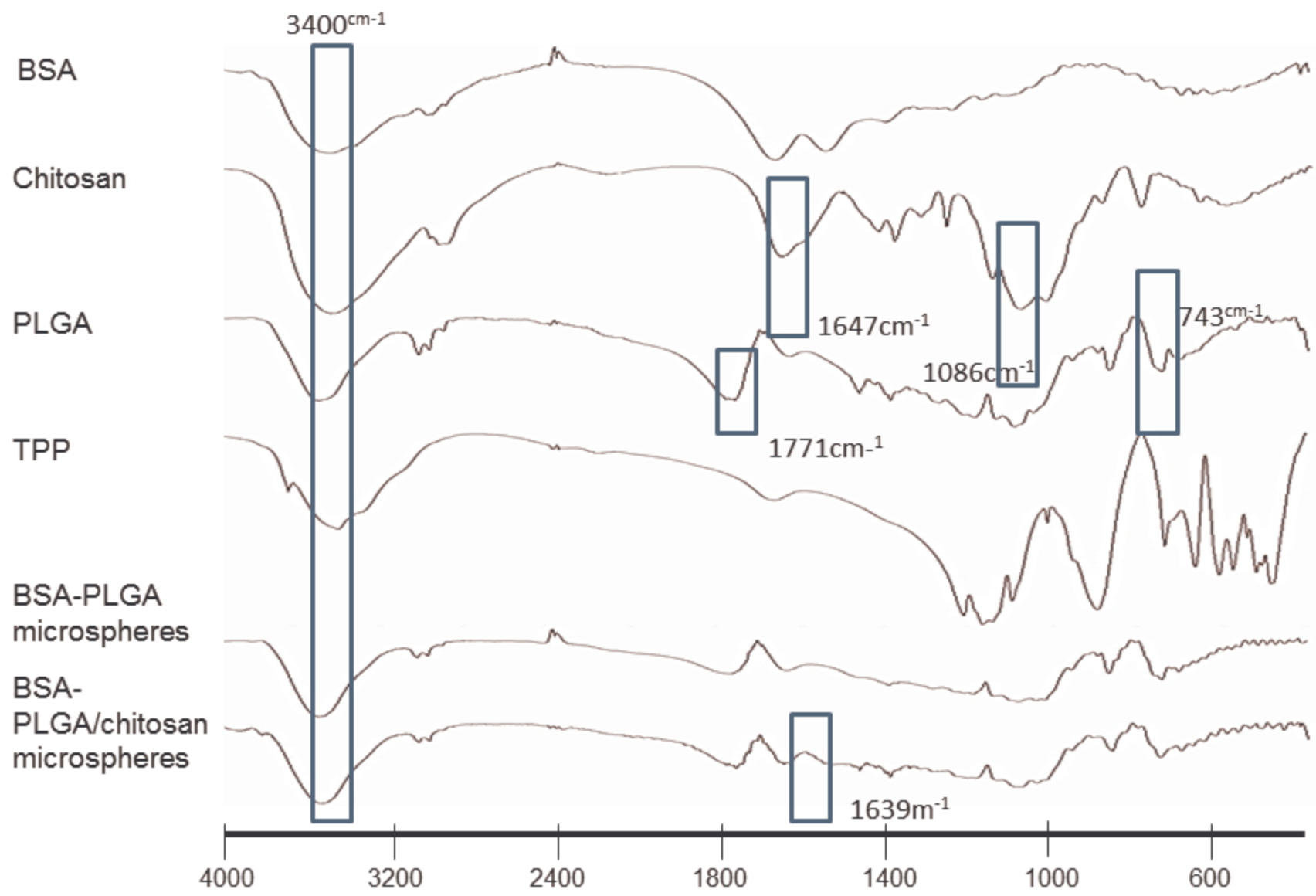
604 Pandey CM, Sharma A, Sumana G, Tiwari I, Malhotra BD 2013. Cationic poly(lactic-co-  
605 glycolic acid) iron oxide microspheres for nucleic acid detection. *Nanoscale* 5: 3800–3807.

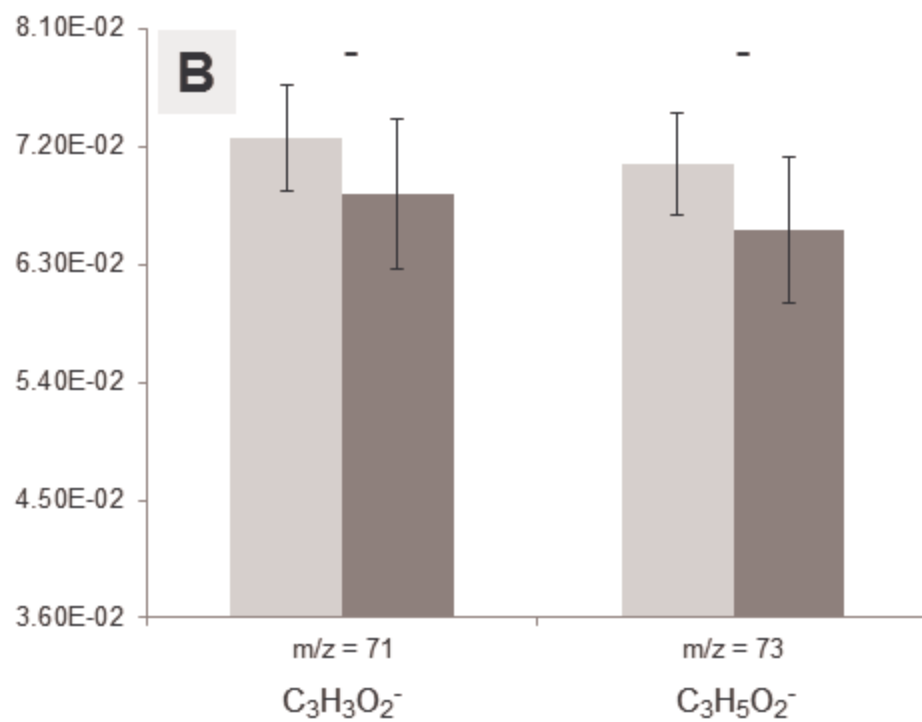
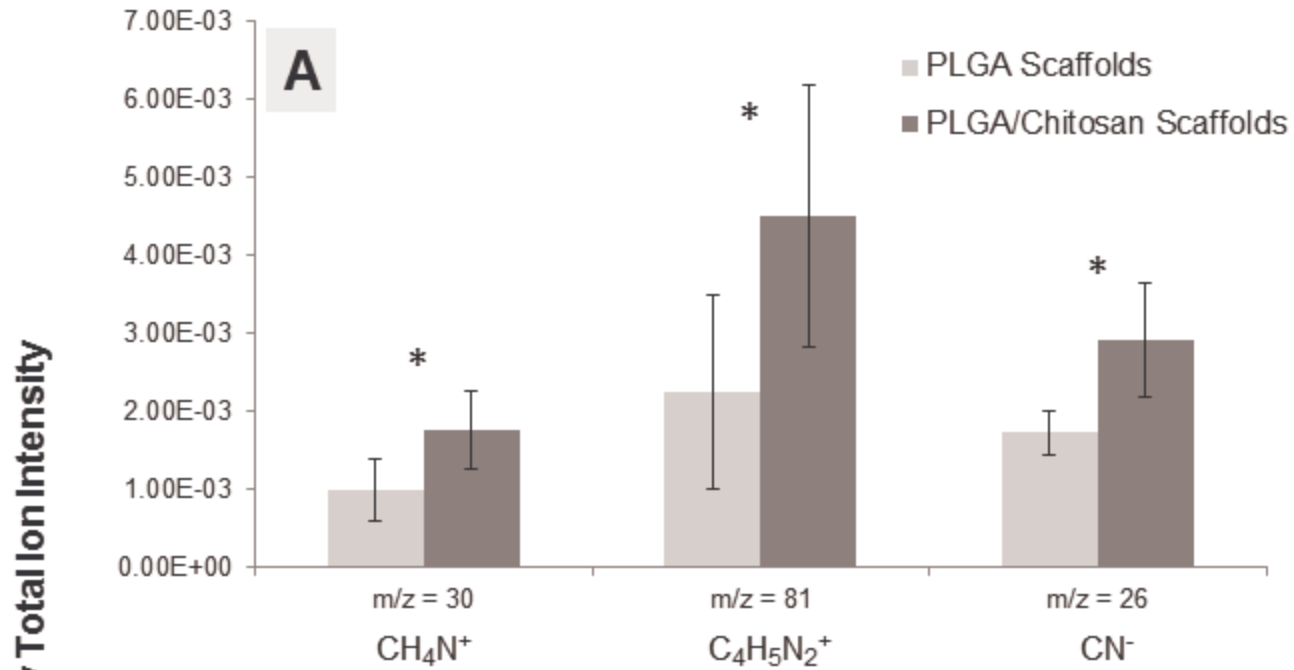
606 Patel ZS, Yamamoto M, Ueda H, Tabata Y, Mikos AG 2008. Biodegradable gelatin  
607 microparticles as delivery systems for the controlled release of bone morphogenetic protein-  
608 2. *Acta Biomater* 4: 1126–1138.

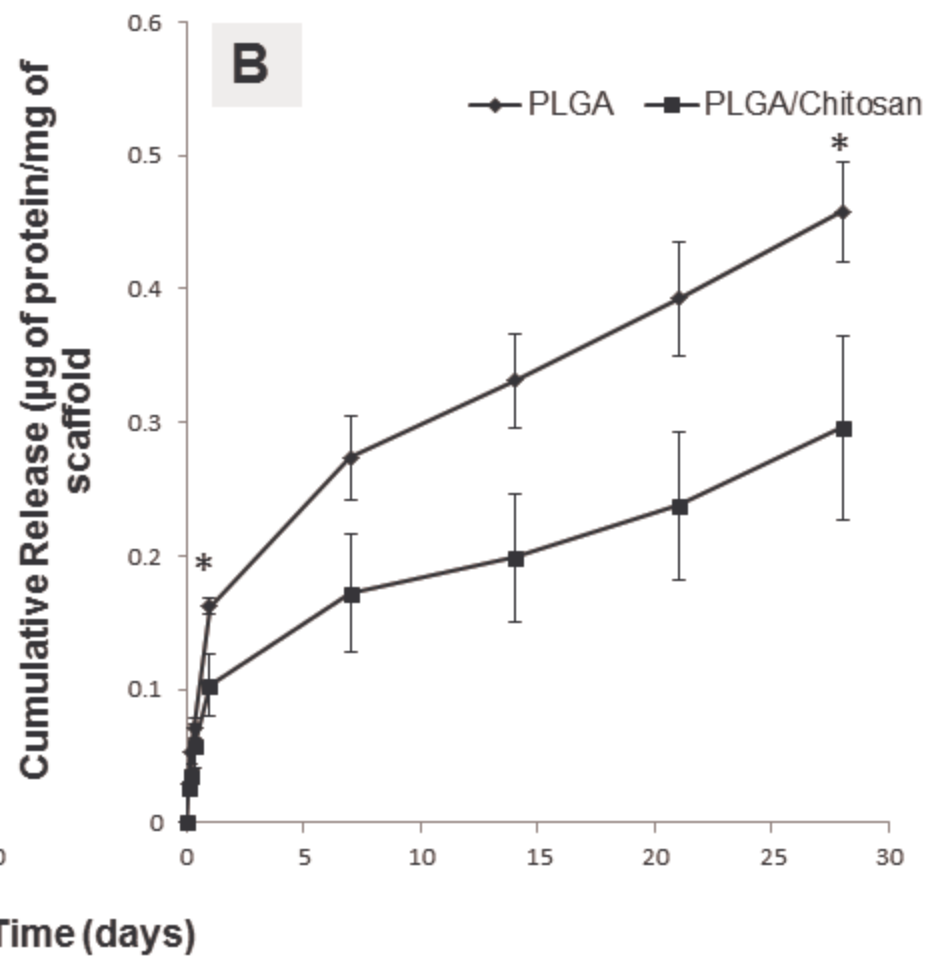
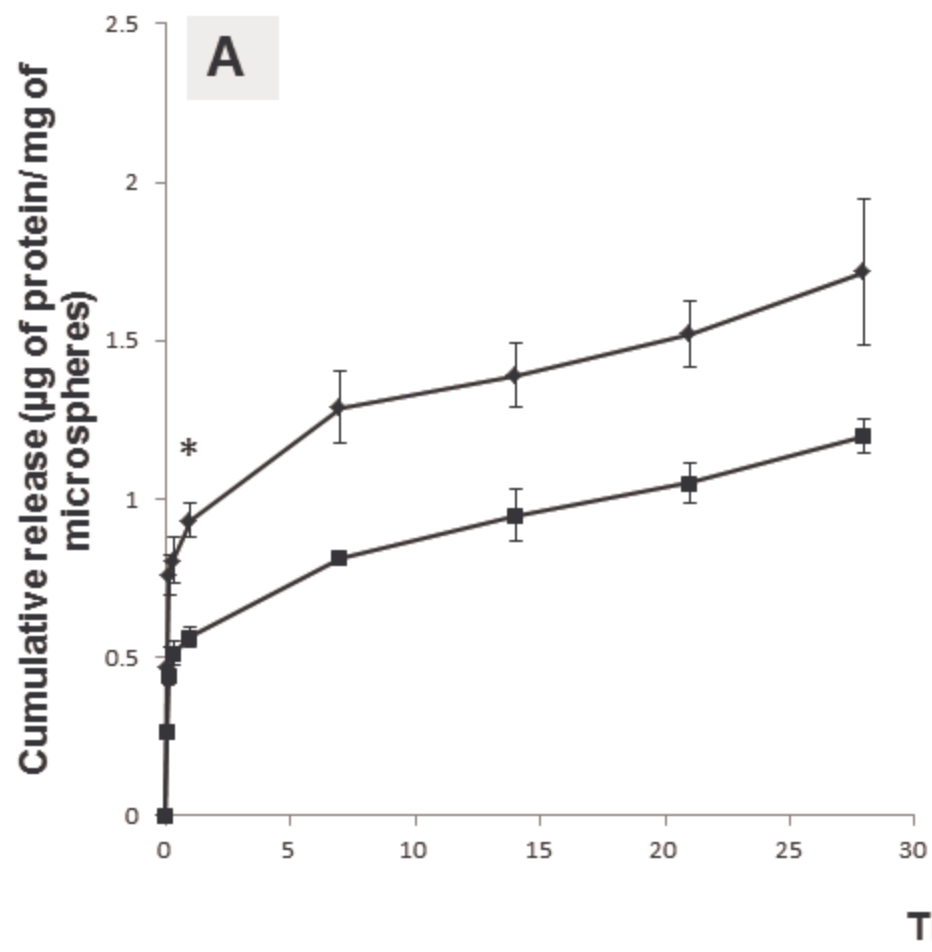
- 609 Puppi D, Chiellini F, Piras a. M, Chiellini E 2010. Polymeric materials for bone and cartilage  
610 repair. *Prog Polym Sci* 35: 403–440.
- 611 Qian L, Zhang H 2013. One-step synthesis of protein-encapsulated microspheres in a porous  
612 scaffold by freeze-drying double emulsions and tuneable protein release. *Chem Commun* 49:  
613 8833–8835.
- 614 Qutachi O, Vetsch JR, Gill D, Cox H, Scurr DJ, Hofmann S, et al. 2014. Injectable and  
615 porous PLGA microspheres that form highly porous scaffolds at body temperature. *Acta*  
616 *Biomater* 10: 5090–5098.
- 617 Rafati A, Boussahel A, Shakesheff KM, Shard AG, Roberts CJ, Chen X, et al. 2012.  
618 Chemical and spatial analysis of protein loaded PLGA microspheres for drug delivery  
619 applications. *J Control Release* 162: 321–329.
- 620 Song K, Liu Y, Macedo HM, Jiang L, Li C, Mei G, Liu T 2013. Fabrication and evaluation of  
621 a sustained-release chitosan-based scaffold embedded with PLGA microspheres. *Mater Sci*  
622 *Eng C* 33: 1506–1513.
- 623 Song K, Liu Y, MacEdo HM, Jiang L, Li C, Mei G, Liu T 2013. Fabrication and evaluation  
624 of a sustained-release chitosan-based scaffold embedded with PLGA microspheres. *Mater Sci*  
625 *Eng C* 33: 1506–1513.
- 626 Stein GS, Lian JB, Owen T a 1990. Relationship of cell growth to the regulation of tissue-  
627 specific gene expression during oseoblast differentiation. *FASEB J* 4: 3111–3123.
- 628 Tao C, Huang J, Lu Y, Zou H, He X, Chen Y, Zhong Y 2014. Development and  
629 characterization of GRGDSPC-modified poly(lactide-co-glycolide acid) porous microspheres  
630 incorporated with protein-loaded chitosan microspheres for bone tissue engineering. *Colloids*  
631 *Surfaces B Biointerfaces* 122: 439–446.
- 632 Tran VT, Benoît JP, Venier Julienne MC 2011. Why and how to prepare biodegradable,  
633 monodispersed, polymeric microparticles in the field of pharmacy? *Int J Pharm* 407: 1–11.
- 634 Vo TN, Kasper FK, Mikos AG 2012. Strategies for controlled delivery of growth factors and  
635 cells for bone regeneration. *Adv Drug Deliv Rev* 64: 1292–1309.
- 636 Wang Y, Shi X, Ren L, Wang C, Wang D-A 2009. Porous poly (lactic-co-glycolide)  
637 microsphere sintered scaffolds for tissue repair applications. *Mater Sci Eng C* 29: 2502–2507.
- 638 Wang Y, Shi X, Ren L, Yao Y, Zhang F, Wang D-A 2010. Poly(lactide-co-glycolide)/titania  
639 composite microsphere-sintered scaffolds for bone tissue engineering applications. *J Biomed*  
640 *Mater Res B Appl Biomater* 93: 84–92.
- 641 White LJ, Kirby GTS, Cox HC, Qodratnama R, Qutachi O, Rose FRAJ, Shakesheff KM  
642 2013. Accelerating protein release from microparticles for regenerative medicine  
643 applications. *Mater Sci Eng C Mater Biol Appl* 33: 2578–2583.

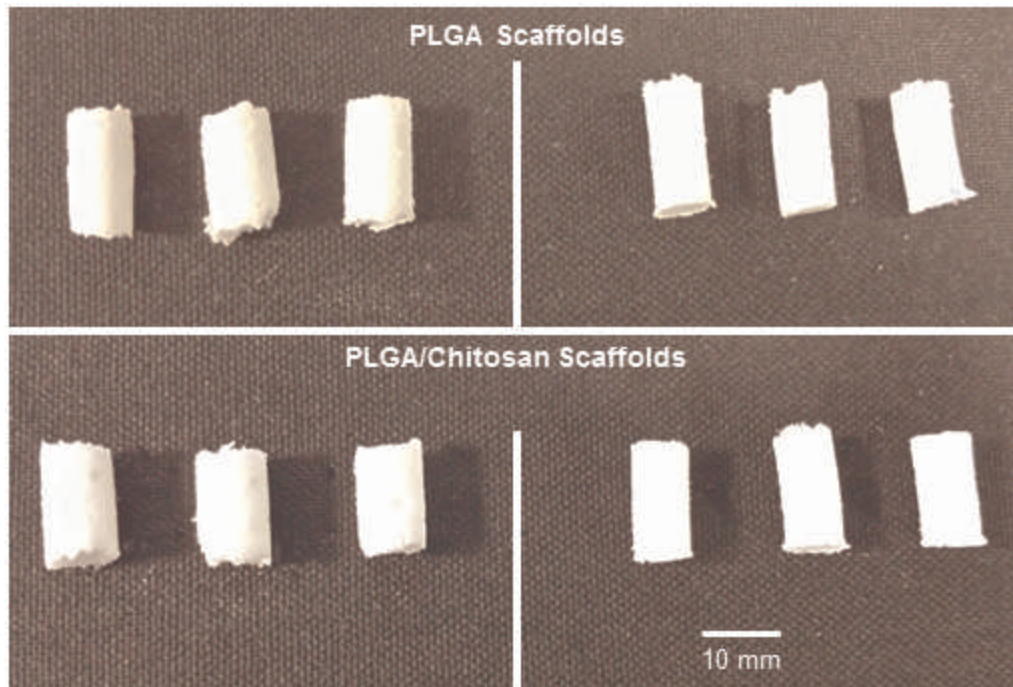
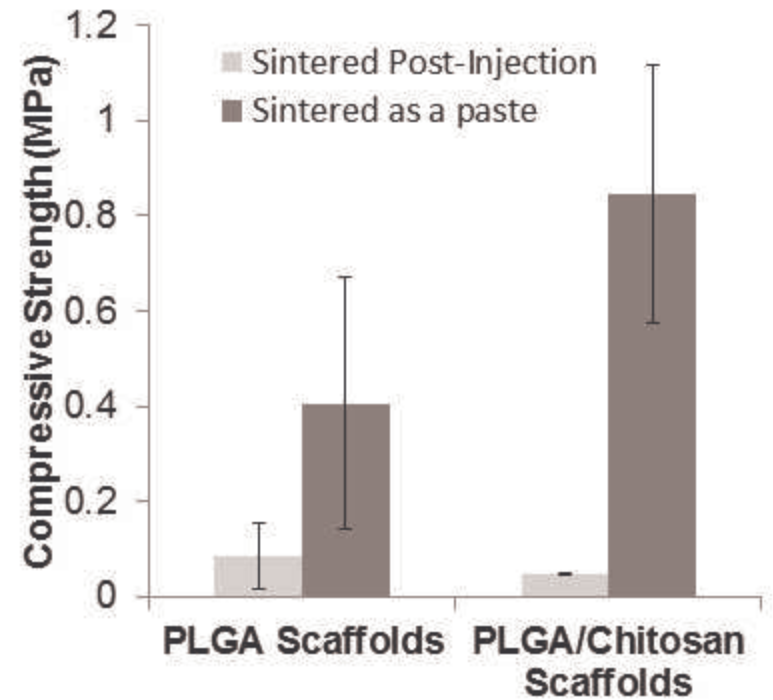
- 644 Yilgor P, Hasirci N, Hasirci V 2010. Sequential BMP-2/BMP-7 delivery from polyester  
645 nanocapsules. *J Biomed Mater Res - Part A* 93: 528–536.
- 646 Yilgor P, Tuzlakoglu K, Reis RL, Hasirci N, Hasirci V 2009. Incorporation of a sequential  
647 BMP-2/BMP-7 delivery system into chitosan-based scaffolds for bone tissue engineering.  
648 *Biomaterials* 30: 3551–3559.
- 649 Yu Y, Chen J, Chen R, Cao L, Tang W, Lin D, et al. 2015. Enhancement of VEGF-Mediated  
650 Angiogenesis by 2- *N*,6- *O* -Sulfated Chitosan-Coated Hierarchical PLGA Scaffolds. *ACS*  
651 *Appl Mater Interfaces* 7: 9982–9990.
- 652 Zeng W, Huang J, Hu X, Xiao W, Rong M, Yuan Z, Luo Z 2011. Ionically cross-linked  
653 chitosan microspheres for controlled release of bioactive nerve growth factor. *Int J Pharm*  
654 421: 283–290.
- 655 Zheng C hong, Liang W 2010. A one-step modified method to reduce the burst initial release  
656 from PLGA microspheres. *Drug Deliv* 17: 77–82.

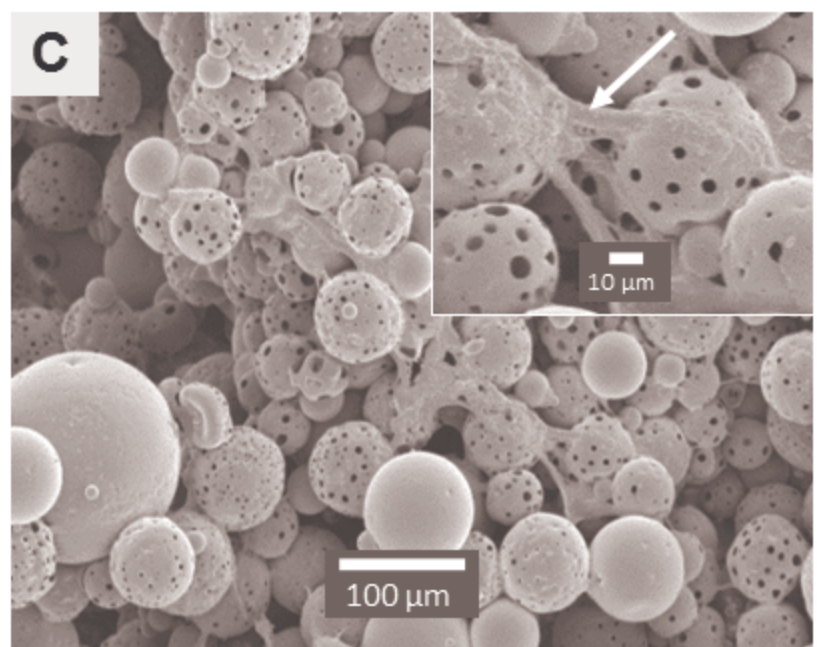
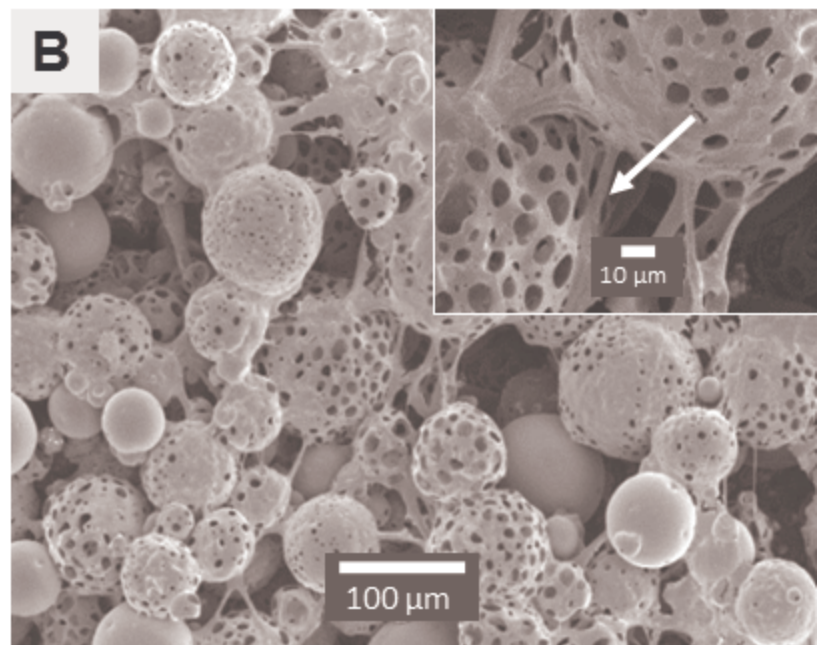
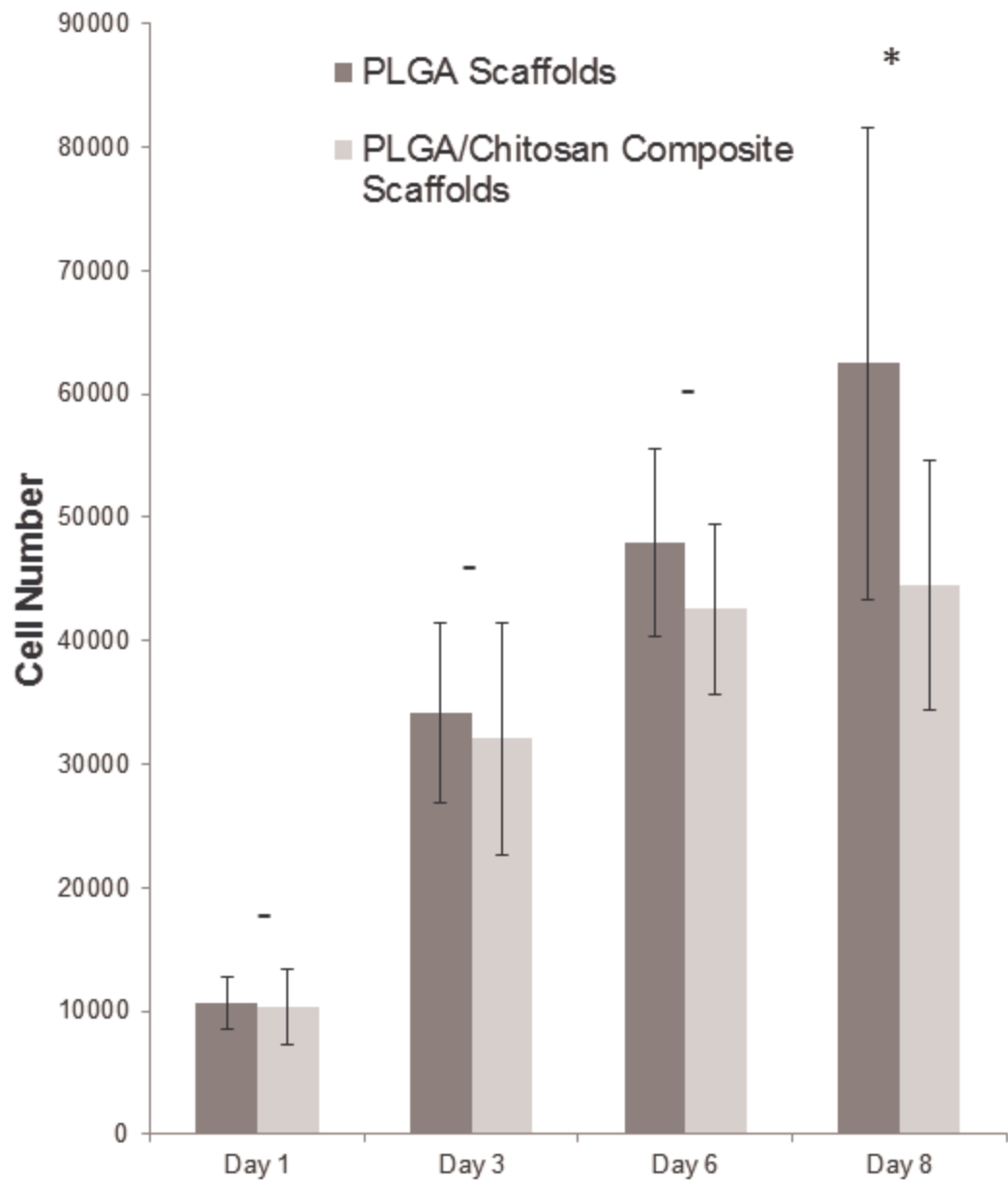


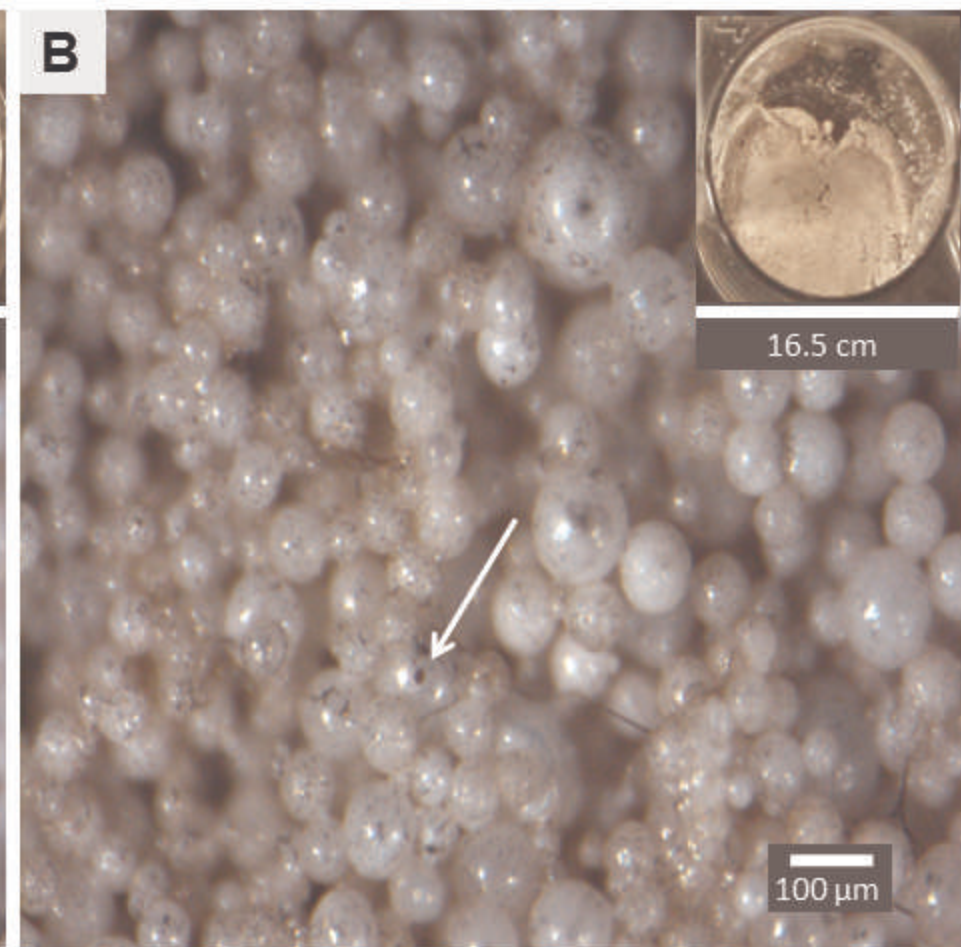
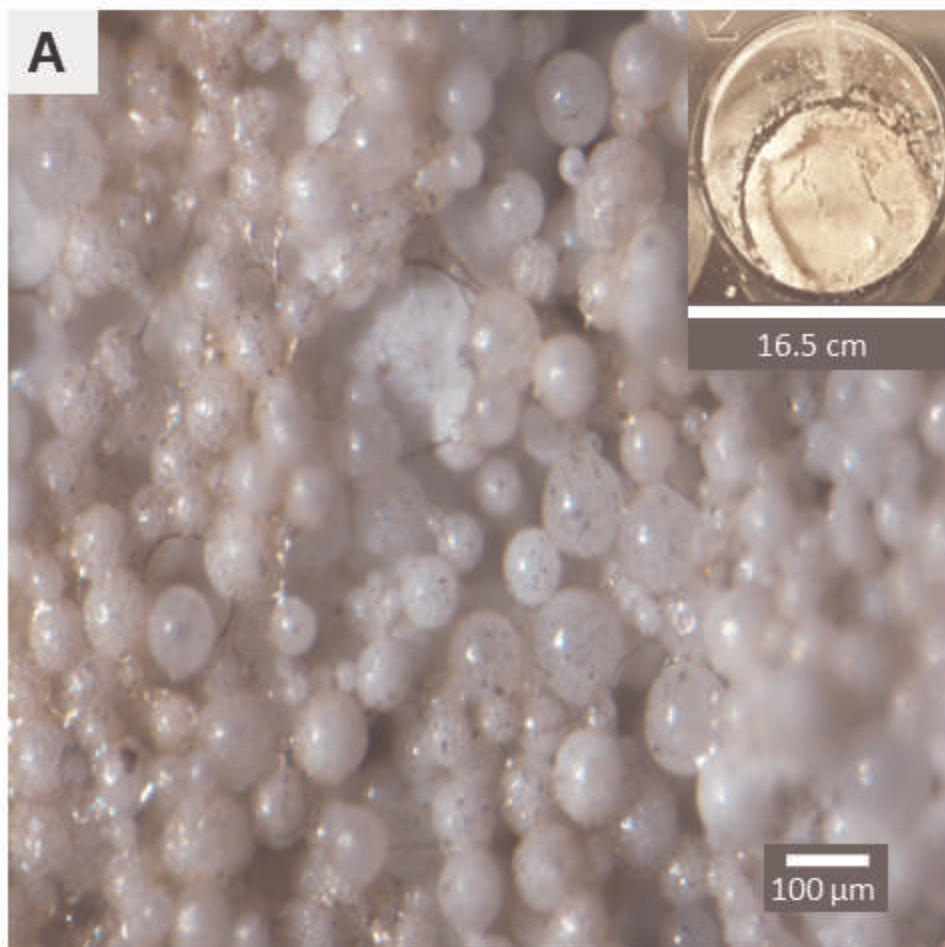


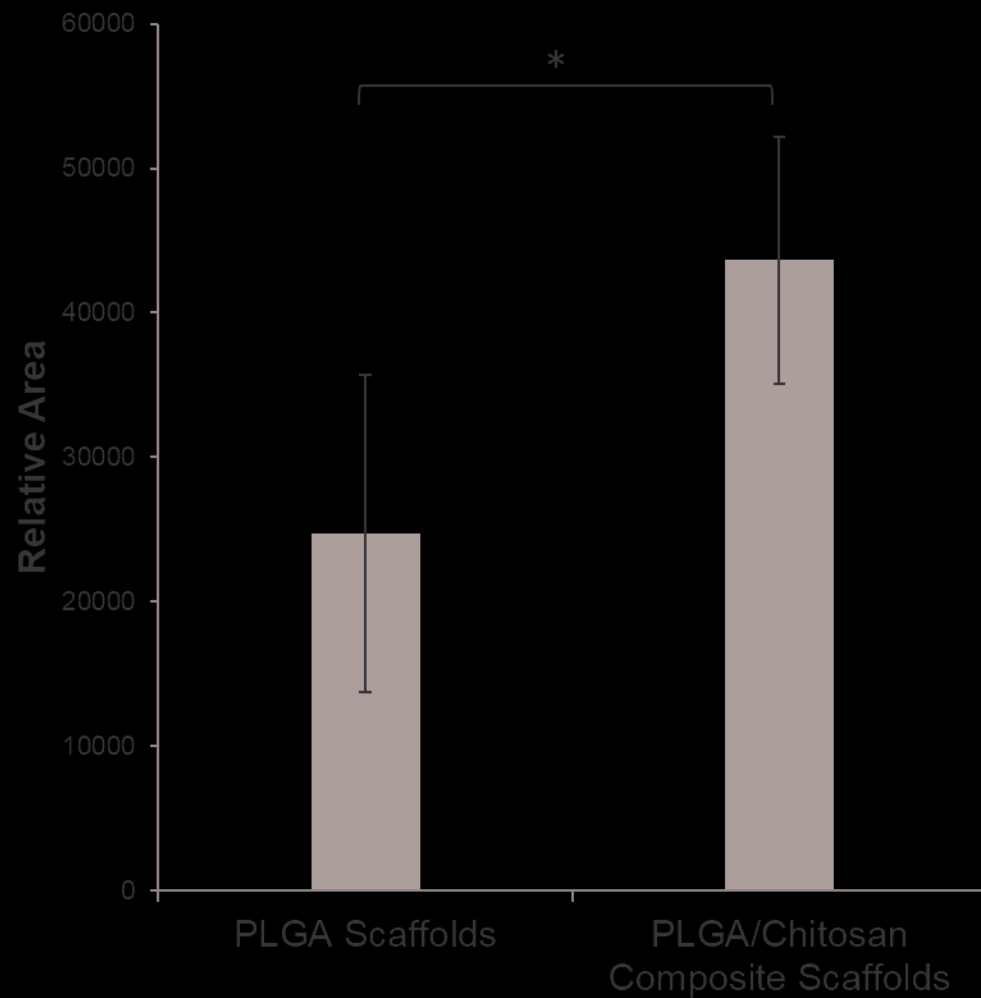
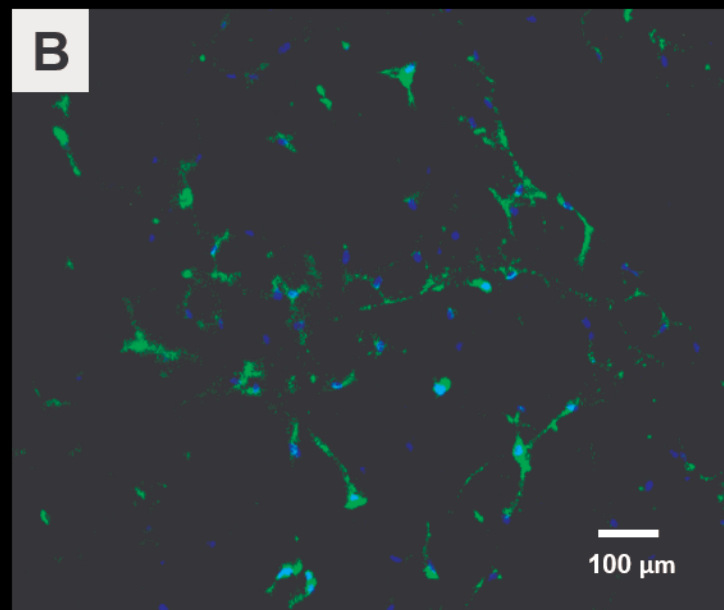




**A****Sintered as a suspension  
post-injection****Sintered as a paste****B**

**A**



**A****B****C**